AIP | Applied Physics Letters

Excitation characteristics of different energy transfer in nanotube-perylene complexes

Friederike Ernst, Timm Heek, Antonio Setaro, Rainer Haag, and Stephanie Reich

Citation: Applied Physics Letters **102**, 233105 (2013); doi: 10.1063/1.4810912
View online: http://dx.doi.org/10.1063/1.4810912
View Table of Contents: http://scitation.aip.org/content/aip/journal/apl/102/23?ver=pdfcov
Published by the AIP Publishing

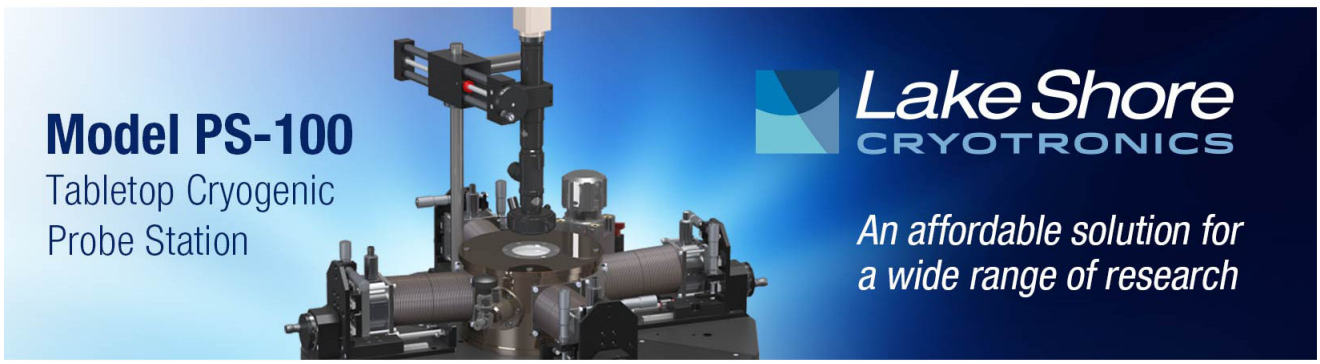

Excitation characteristics of different energy transfer in nanotube-perylene complexes

Friederike Ernst,[1,a)] Timm Heek,[2] Antonio Setaro,[1] Rainer Haag,[2] and Stephanie Reich[1]
[1]*Institut für Experimentalphysik, Freie Universität Berlin, Germany*
[2]*Institut für Chemie und Biochemie, Freie Universität Berlin, Germany*

(Received 12 March 2013; accepted 28 May 2013; published online 12 June 2013)

We report the properties of perylene-nanotube complexes that form efficient energy transfer systems. Most perylene-derivatives yield similar ratios between transfer and direct luminescence (0.66 ± 0.04). The photoluminescence spectra of the free compounds and the transfer complex are similar indicating that perylene and nanotubes act as separate systems. A further increase in interaction yields 40% higher transfer rates and luminescence excitation spectra that indicate a change in stacking of the perylene on the nanotube wall. All measurements are consistent with a transfer mechanism based on a dipole-dipole interaction at a distance much smaller than the Förster radius. © *2013 AIP Publishing LLC*. [http://dx.doi.org/10.1063/1.4810912]

Quantum confinement gives single walled carbon nanotubes (SWNTs) highly desirable macroscopic properties, such as ballistic transport. At the same time, confinement restricts the part of the electromagnetic spectrum a nanotube interacts with.[1–4] This is a major drawback for any application that relies on interaction with light, for instance use in photovoltaic devices and optical transistors. The formation of complex quantum systems with multiple functional units is thus an active area of research.[5–7] Particularly, the combination of nanotubes with chromophores holds great promise: The dye constitutes the part that interacts with light efficiently, while the nanotube acts as a nanolead.[8] Many chromophores with extended π orbitals can stack on carbon nanotubes non-covalently, preserving the nanotubes' desirable optoelectronic properties. The close proximity between nanotube and dye permits an exciton created in the dye to be transferred into the nanotube.[9–11]

SWNT-dye energy transfer complexes have been created in two distinct ways, through micelle swelling[10,12,13] and through the direct incorporation of chromophoric units into the surfactant. The second approach is predicated on a single-step functionalization process; the chromophoric unit is integrated into the surfactant.[11,14–16] We demonstrated this recently for a class of perylene based surfactants.[16] Up to now, energy-transfer studies concentrated on a given combination of dye and nanotube. The transfer was analyzed for individual excitation energies. Now the question arises of how to optimize the nanotube-dye interaction. Understanding the transfer mechanism requires systematical excitation energy dependent studies.

In this paper, we explore the energy transfer mechanism by evaluating the differences in the transfer characteristics for various perylene-nanotube complexes. We find a strong dependence on stacking arrangement between chromophore and nanotube, as well as an energetic fine structure. The transfer efficiency is determined by the adsorption morphology. For one group of compounds, the chemical structure precludes closer stacking, resulting in transfer efficiencies (0.66 ± 0.04). The more closely bound compounds displayed 40% higher transfer efficiencies. The photoluminescence excitation (PLE) spectra of the nanotube-dye complexes formed with the more closely stacking compounds show features indicative of a change in the perylene adsorption pattern on the nanotube walls.

The studied surfactants comprised a perylene core, a unit for water solubility, and alkyl chains of varying characteristics for individualization and suspension of the nanotubes. We previously showed that these molecules are surfactants and form energy transfer complexes with nanotubes.[16] The chemical structures of the five molecules that resulted in energy transfer complexes are given in Fig. 1(a). The electronic structure of the molecules is determined by their identical chromophore core. For the experimental preparation of all molecule-nanotube complexes, see Ref. 16. The samples in this work were prepared with a surfactant concentration of $6 \cdot 10^{-5}$M of surfactant and 0.11 g/l of HiPco SWNTs (Unidym, batch SP0295). Samples were tip sonicated and centrifuged at 30 000 g. Only the supernatant was used in the optical measurements.

We gain experimental access to the energy transfer complexes through PLE spectra, which resolve the excitation channels of the complexes. PLE measurements were conducted in a Horiba NanoLog system. The photoluminescence (PL) spectra were excited with a Xe short arc lamp, from which a single excitation line was selected using a monochromator with two mechanically coupled gratings (1200 grooves/mm, blazed at 500 nm). The PL intensity was recorded with a nitrogen-cooled InGaAs detector (IR) and a photomultiplier (vis). PL/PLE maps were created by joining PL spectra with an excitation energy resolution of 2 nm.

Figure 1(b) schematically depicts the energy transfer from the chromophore to the tube. Combined photoluminescence and photoluminescence excitation maps of the constituent systems as well as the combined nanotube-chromophore complex are given in Fig. 2 for the example of molecule **B**. Figure 2(a) shows the map for compound **B** in water, (b) the PLE map for pristine nanotubes. The peaks correspond to the characteristic E_{22} (excitation) and E_{11} (emission) transition

a)f.ernst@fu-berlin.de

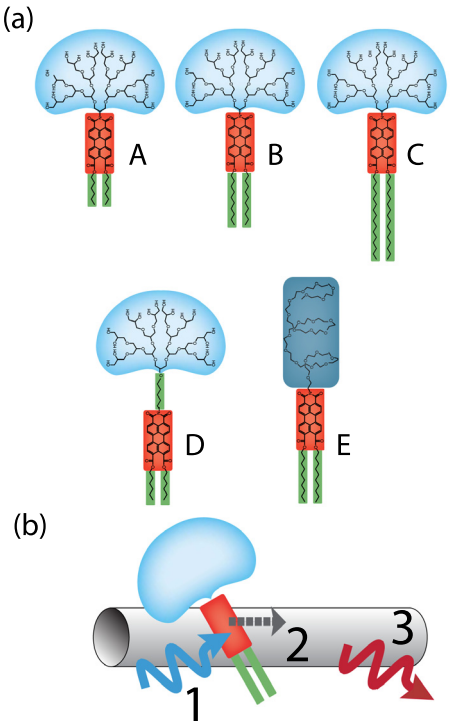

FIG. 1. (a) Chemical structures of the chromophoric components of the energy transfer complexes. All molecules **A** - **E** comprise a dye core (red), alkyl chains (green), and a hydrophilic dendron (light blue) or linear polyethyleneglycol chain (dark blue) for water solubility. (b) Schematic of the energy transfer process in the chromophore-nanotube complex.

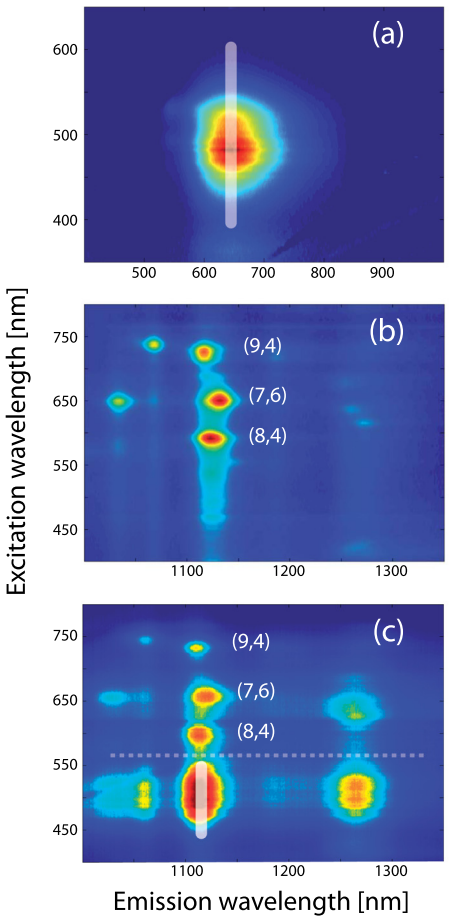

FIG. 2. (a) PLE map for compound **B** in water. (b) PLE map for pristine nanotubes in aqueous suspension; note the absence of all energy transfer peaks below an excitation wavelength of 550 nm. (c) PLE map for nanotubes functionalized with compound **B**. The peaks above the dashed gray line correspond to the emission of the nanotubes after direct excitation at their E_{22} transition energies. The peaks below the gray line correspond to the emission of the same tubes after the indirect excitation via the adsorbed molecule **B**.

energies of various nanotube chiralities (see labels).[4] In the PLE map of the combined system, Fig. 2(c), the same peaks are observed for direct excitation. Additionally, an emission from the nanotubes is seen after the excitation of the adsorbed compound **B** (broad peaks below the dashed gray line). The excitation wavelength of the energy transfer peaks corresponds to the excitation wavelength of the adsorbed molecule, while the emission wavelength corresponds to the E_{11} emission of the nanotubes, Fig. 1(b). The area marked by the vertical gray bar around 1130 nm in Fig. 2(c) is thus the emission of nanotubes (9,4), (7,6), and (8,4) after excitation transfer through perylene-derivative **B**.

The transfer rate between energy donor (perylene) and acceptor (nanotube) is evaluated by the quenching $\gamma_{D\to A}/\gamma_D = 10^{-4}$ of the perylene luminescence, Fig. 2(a).[17] We experimentally observe a transfer efficiency[11]

$$E = 1 - \frac{\gamma_{D\to A}}{\gamma_D} = 1 - 10^{-4} \simeq 1, \tag{1}$$

where γ_D is the excitation rate of the donor and $\gamma_{D\to A}$ is the transfer rate from donor to acceptor. This value is in line with time-resolved measurements on comparable porphyrin-nanotube systems that yielded $\tau_{D\to A}/\tau_D < 10^{-4}$, with τ_D the excitation life time in the donor, and $\tau_{D\to A}$ the excitation life time in the donor in the presence of the acceptor.[18]

We evaluate the ratio η between the transfer and the direct luminescence intensities

$$\eta = \frac{I_{\text{transfer}}}{I_{\text{direct (9,4)}} + I_{\text{direct (7,6)}} + I_{\text{direct (8,4)}}}, \tag{2}$$

where $I_{\text{direct(n,m)}}$ is the luminescence intensity after resonantly exciting the (n, m) tube at its E_{22} transition energy, and I_{transfer} is the combined luminescence of the (9,4), (7,6), and (8,4) tubes after an excitation of the perylene at 480 nm and subsequent energy transfer. While the three tubes have distinct E_{22} energies, their E_{11} emission energies are very similar. When excited via the dye adsorbate, they have only one combined energy transfer peak. The results are listed in Table I. η is 0.66 ± 0.04 for compounds **A**, **B**, and **C** and 40% higher for **D** and **E**.

η depends on the coverage of the tubes with dye molecules and allows a rough estimate of the absolute coverage of the tubes in perylene dye. The oscillator strength per carbon atom is ~0.01 for nanotubes and ~0.1 for perylene.[19,20] For full coverage of the carbon nanotube, one would expect

TABLE I. Ratio η between direct and transfer luminescence intensities for the (9,4), (7,6), and (8,4) tubes.

Compound	H	Compound	η
A	0.65 ± 0.03	**D**	$\mathbf{0.93 \pm 0.01}$
B	0.67 ± 0.02	**E**	$\mathbf{0.90 \pm 0.02}$
C	0.66 ± 0.03		

TABLE II. Förster radii R_0 for tubes (9,4), (7,6), and (8,4) and resulting nanotube-chromophore distances R.

Chirality	Tube radius (nm)	R_0 (nm)	R (nm)
(9,4)	0.45	5.4	1.2
(7,6)	0.44	6.6	1.5
(8,4)	0.42	5.3	1.2

$\eta \approx 10$, since for $E \approx 1$, practically every excitation is transferred into nanotubes. From $\eta \approx 1$, we conclude that roughly 10% of the nanotube wall is covered in dye. This is a fairly dense coverage, as the dye constitutes only a small part of the surfactant, see Fig. 1. To directly confirm this estimate, cryo-TEM measurements will be conducted.[21]

To further analyze the perylene-nanotube complex, we assume Förster-type energy transfer within the dipole approximation. The Förster radius R_0 is the distance at which half the luminescence of the donor is quenched by the acceptor and is given by[17]

$$R_0 = \left[\Phi_D \cdot \frac{9c\kappa^2}{64\pi^2 n^4} \int_0^\infty f_D(\lambda) f_A(\lambda) \lambda^2 \mathrm{d}\lambda\right]^{1/6}. \quad (3)$$

R_0 depends on the spectral overlap between the donor emission $f_D(\lambda)$ and the acceptor absorption $f_A(\lambda)$, the quantum efficiency of the donor Φ_D, the refractive index of the solvent n, and the relative orientation of the dipoles to each other κ. For randomly oriented dipoles, $\langle\kappa\rangle^2 = 2/3$.

Figure 2 shows that in the emission region of the dye, 520–700 nm, the (9,4), (7,6), and (8,4) tubes have different absorbance spectra, $f_A(\lambda)$. Consequently, the three tubes have slightly different Förster radii R_0. Using Eq. (3), we determine the Förster radii for compound **B** as listed in Table II. The Förster radii are then used to determine the mean distance R between perylene and nanotube[17]

$$R = R_0 \cdot \sqrt[6]{\frac{1}{E} - 1} \approx \mathrm{R}_0 \cdot \sqrt[6]{\frac{\gamma_{\mathrm{D}\to\mathrm{A}}}{\gamma_{\mathrm{D}}}} = 0.22 \cdot R_0. \quad (4)$$

The mean distance, Table II, implies a separation between nanotube wall and perylene of ~0.9 nm. This is not much larger than the van-der-Waals distance in π-π stacking (0.34 nm). We note that the point-dipole approximation overestimates the dipole-dipole coupling and transfer rates in one dimensional systems.[22] The stacking might be even closer than estimated here. There is only one spatial arrangement in which this proximity between nanotube and the dye core of the molecules can be attained; by direct stacking of the perylene on the tube wall. The corresponding analysis for the perylene-tube distance of compound **C** yielded very similar results to compound **B**. Unfortunately, the high amount of free dye prohibited measurements of the Förster radius for **A**, **D**, and **E**.[16] Instead, we will use the transfer efficiency η

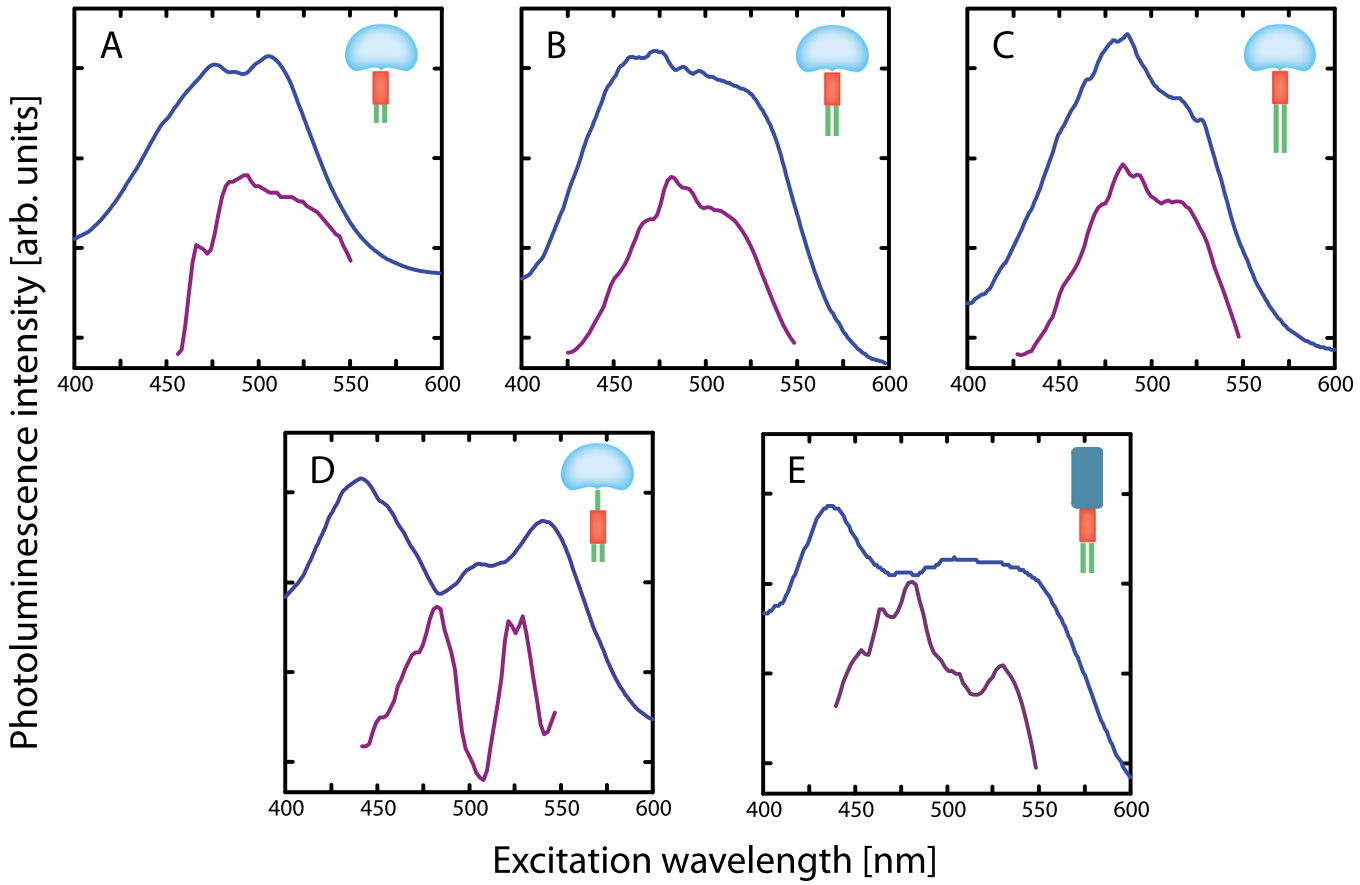

FIG. 3. PL intensity (blue, top) of the indicated molecules A-E in dependence of the excitation wavelength. The PLE line was sampled at the wavelength for which the dye's emission is maximal, as illustrated by the gray bar in the PLE map in Fig. 2(a). The PLE line of the molecule-nanotube complexes (purple, bottom) was sampled in the emission window of the (9,4), (7,6), and (8,4) tubes, as indicated by the gray bar in Fig. 2(c). All data are offset for clarity.

and PLE spectra to gain insight into the geometry and energy-transfer channels.

The molecules fell into two groups of slightly lower (**A**, **B**, **C**) and higher (**D**, **E**) efficiencies, see Table I. We argue the higher transfer rate of **D** and **E** to be due to a closer stacking on the tube. This is further supported by the PLE spectra of the energy transfer complexes. In Fig. 3, we show the PLE spectra of the energy transfer peak around 1130 nm for the various surfactant molecules (purple). The emission energies of the three chiralities contributing to this energy transfer peak, i.e., (9,4), (7,6), and (8,4), are slightly different. The PLE line for the complexes was averaged over the emission range 1105–1145 nm.[23] The PLE spectra (blue) of the molecules alone were evaluated at the maximum emission of the molecule, as illustrated by the vertical gray line in the PLE map of compound **B** in Fig. 2(a).[24,30]

For complexes formed with molecules **A**-**C**, Fig. 3, the PLE spectra mimic the PLE spectra of the dye alone. Note that the PL intensity for **A**-nanotube complexes does not fall as far as would be expected for longer wavelengths; there is still considerable emission at 550 nm. Compound **A** debundles nanotubes far less efficiently than **B** and **C**,[16] resulting in larger bundles and broader PL peaks.[25] The PLE spectra of nanotube complexes with **D** and **E**, in contrast, differ from the dye alone. Moreover, the spectral form changes drastically: The continuous excitation spectrum divides into two distinct peaks of which the high-energy peak red shifts compared to free compound, and the low energy peak blue shifts. We attribute this to different stacking characteristics between nanotube and perylene derivatives dye. A geometry dependent change in the spectra of perylene bisimide stacks is reported in the literature.[26–29] We assume similar characteristics also for the stacking between perylene bisimide and carbon nanotubes. Following Ref. 26, the relative intensities of the two broad peaks in the PLE spectra in compounds **A**-**E** indicate a predominant orientation 60°-80° between the dipole of the perylene and the nanotube. The peak splitting observed for **D** and **E** when compared with **A**-**C** is characteristic of a smaller distance between the dye and the tube in good agreement with our evaluation of the transfer rates. An alternative explanation for the splitting is the tilting of the perylene on the nanotube wall, which we consider less likely.[26] Compounds **D** and **E** differ from the other molecules under study in that the perylene core is not only attached to alkyl chains on one side but also possesses an alkyl or polyethyleneglycol chain on the other side, Fig. 1(a). This makes the perylene unit much more flexible as compared to the other compounds. It permits optimized stacking and explains the increased efficiency of the energy transfer for compounds **D** and **E** and the differences in the PLE spectra.

The PLE spectra in Fig. 3 display a fine structure. Such features were also predicted in simulations on the stacking geometry of perylene dyes.[26] It is owed to a vibrational coupling between the electronic bands. In principle, these vibrational coupling modes can be used for extracting the electronic coupling strength between nanotube and dye. In practice, this is difficult because the fine structure may result from vibrational motion, electronic coupling, or both.[26]

In conclusion, we demonstrated that nanotube-perylene energy transfer complexes can be described with a Förster like energy transfer with a Förster radius $R_0 \approx 6$nm. The nanotube-compound distance is well below R_0. The chromophore coverage of the nanotubes is on the order of ~10%. Variation in the morphology of the surfactant results in a varying adsorption geometry, which strongly influenced the electronic properties of the energy transfer complexes. Understanding the physical mechanisms, underlying close-range energy transfer complexes is crucial for the advancement of quantum engineering applications. To elucidate the physical mechanism behind the fine structure in the energy transfer spectrum, we will pursue density functional theory calculations.

We gratefully acknowledge the financial support of the European Research Council (Grant No. 210642) and the German Research Foundation (DFG via SFB 658, subprojects A6 and B7), and thank Sebastian Heeg, Benjamin Hatting, Mareen Gläske, and Pascal Blümmel for productive discussions.

[1]S. Reich, C. Thomsen, and J. Maultzsch, *Carbon Nanotubes* (Wiley-VCH, 2004).
[2]A. Jorio, M. S. Dresselhaus, and G. Dresselhaus, *Carbon Nanotubes—Advanced Topics in the Synthesis, Structure, Properties, and Applications* (Springer, 2008).
[3]M. J. O'Connell, S. M. Bachilo, C. B. Huffman, V. C. Moore, M. S. Strano, E. H. Haroz, K. L. Rialon, P. J. Boul, W. H. Noon, C. Kittrell, J. Ma, R. H. Hauge, R. B. Weisman, and R. E. Smalley, Science **297**, 593 (2002).
[4]S. M. Bachilo, M. S. Strano, C. Kittrell, R. H. Hauge, R. E. Smalley, and R. B. Weisman, Science **298**, 2361 (2002).
[5]E. Kymakis and G. A. J. Amaratunga, Appl. Phys. Lett. **80**, 112 (2002).
[6]P. W. Barone, R. S. Parker, and M. S. Strano, Anal. Chem. **77**, 7556 (2005).
[7]S. D. Stranks, J. K. Sprafke, H. L. Anderson, and R. J. Nicholas, ACS Nano **5**, 2307 (2011).
[8]P. Avouris, M. Freitag, and V. Perebeinos, Nat. Photonics **2**, 341 (2008).
[9]A. Nish, J.-Y. Hwang, J. Doig, and R. J. Nicholas, Nanotechnology **19**, 095603 (2008).
[10]C. Roquelet, J.-S. Lauret, V. Alain-Rizzo, C. Voisin, R. Fleurier, M. Delarue, D. Garrot, A. Loiseau, P. Roussignol, J. A. Delaire, and E. Deleporte, ChemPhysChem **11**, 1667 (2010).
[11]F. Ernst, T. Heek, A. Setaro, R. Haag, and S. Reich, Adv. Funct. Mater. **22**, 3921 (2012).
[12]G. Magadur, J.-S. Lauret, V. Alain-Rizzo, C. Voisin, P. Roussignol, E. Deleporte, and J. A. Delaire, ChemPhysChem **9**, 1250 (2008).
[13]C. Roquelet, D. Garrot, J. S. Lauret, C. Voisin, V. Alain-Rizzo, P. Roussignol, J. A. Delaire, and E. Deleporte, Appl. Phys. Lett. **97**, 141918 (2010).
[14]C. Backes, C. D. Schmidt, K. Rosenlehner, F. Hauke, J. N. Coleman, and A. Hirsch, Adv. Mater. **22**, 788 (2010).
[15]F. Ernst, T. Heek, R. Haag, S. Reich, and A. Setaro, Phys. Status Solidi B **249**, 2465 (2012).
[16]F. Ernst, T. Heek, A. Setaro, R. Haag, and S. Reich, J. Phys. Chem. C **117**, 1157 (2013).
[17]P. Wu and L. Brand, Anal. Biochem. **218**, 1 (1994).
[18]D. Garrot, B. Langlois, C. Roquelet, T. Michel, P. Roussignol, C. Delalande, E. Deleporte, J.-S. Lauret, and C. Voisin, J. Phys. Chem. C **115**, 23283 (2011).
[19]F. Schöppler, C. Mann, T. C. Hain, F. M. Neubauer, G. Privitera, F. Bonaccorso, D. Chu, A. C. Ferrari, and T. Hertel, J. Phys. Chem. C **115**, 14682 (2011).
[20]Y. Zhao, A.-M. Ren, J.-K. Feng, and C.-C. Sun, J. Chem. Phys. **129**, 014301 (2008).
[21]Based on previous measurements of absorbance and residual PL emission of the perylene derivatives as a function of concentration, Figures 2 (absorbance) and 4 (residual PL) of Ref. 11, we have no reason to suspect self-quenching.

[22]C. Y. Wong, C. Curutchet, S. Tretiak, and G. D. Scholes, J. Chem. Phys. **130**, 081104 (2009).
[23]The same analysis was done for the (9,5), (10,3), and (11,1) tubes (which emit at ∼1280 nm), yielding identical results. See supplemental material at http://dx.doi.org/10.1063/1.4810912 for the corresponding PLE spectra.
[24]All spectra were recorded at low optical densities to avoid artifacts. While the compounds do not have a critical micellar concentration, they stack in solution even at low molarities, resulting in the differences in the PLE spectra. (Ref. 30).
[25]P. Tan, A. Rozhin, T. Hasan, P. Hu, V. Scardaci, W. Milne, and A. Ferrari, Phys. Rev. Lett. **99**, 137402 (2007).
[26]J. Seibt, P. Marquetand, V. Engel, Z. Chen, V. Dehm, and F. Würthner, Chem. Phys. **328**, 354 (2006).
[27]F. Würthner, Z. Chen, V. Dehm, and V. Stepanenko, Chem. Commun. **4**, 1188 (2006).
[28]R. F. Fink, J. Seibt, V. Engel, M. Renz, M. Kaupp, S. Lochbrunner, H.-M. Zhao, J. Pfister, F. Würthner, and B. Engels, J. Am. Chem. Soc. **130**, 12858 (2008).
[29]F. Würthner, T. E. Kaiser, and C. R. Saha-Möller, Angew. Chem., Int. Ed. **50**, 3376 (2011).
[30]T. Heek, J. Nikolaus, R. Schwarzer, C. Fasting, P. Welker, K. Licha, A. Herrmann, and R. Haag, Bioconjugate Chem. **24**, 153 (2013).